Science Advances

AAAS

advances.sciencemag.org/cgi/content/full/3/3/e1602557/DC1

Supplementary Materials for

Room temperature multiplexed gas sensing using chemical-sensitive 3.5-nm-thin silicon transistors

Hossain Mohammad Fahad, Hiroshi Shiraki, Matin Amani, Chuchu Zhang, Vivek Srinivas Hebbar, Wei Gao, Hiroki Ota, Mark Hettick, Daisuke Kiriya, Yu-Ze Chen, Yu-Lun Chueh, Ali Javey

Published 24 March 2017, *Sci. Adv.* **3**, e1602557 (2017)
DOI: 10.1126/sciadv.1602557

This PDF file includes:

Supplementary Materials

S1. Sensor characteristics of an unfunctionalized CS-FET sensor

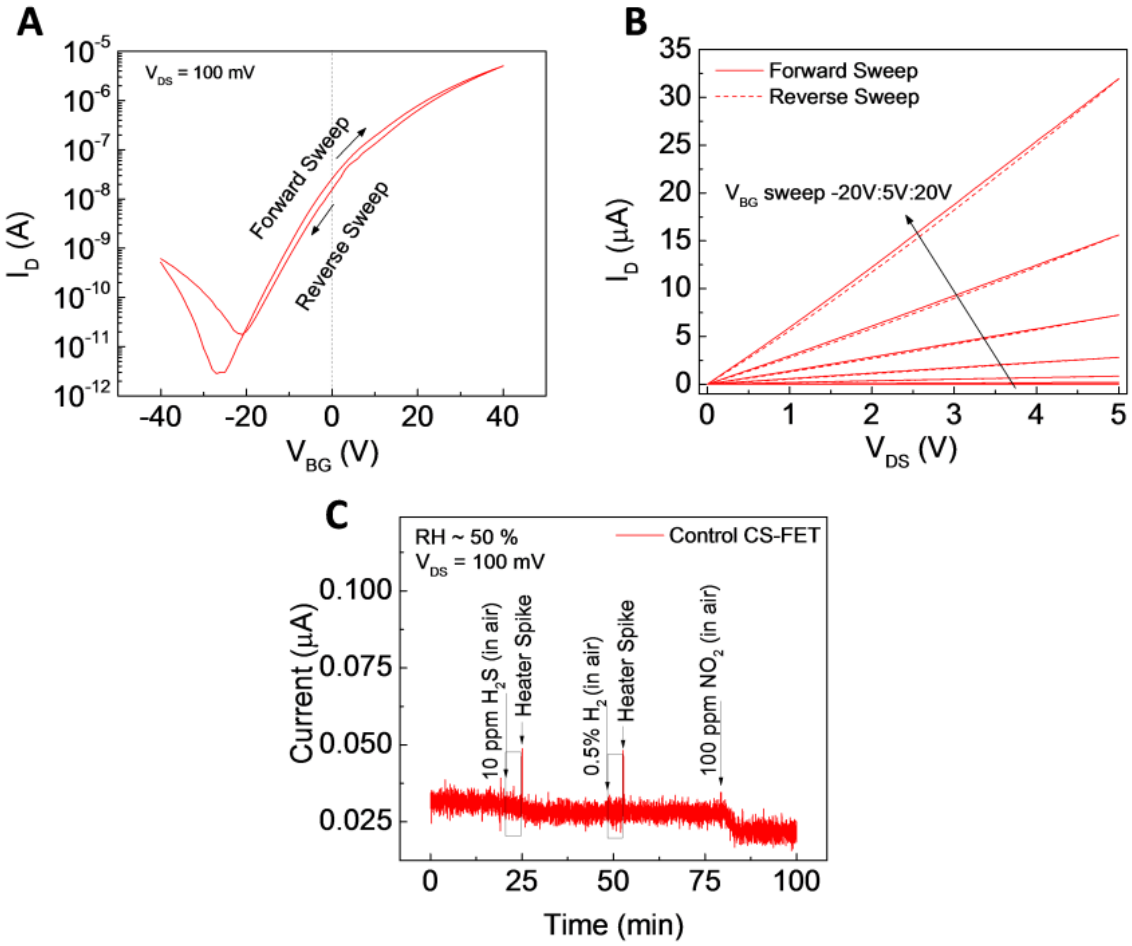

fig. S1. Properties of a control CS-FET without any sensing film. (**A**) Double sweep electrical transfer curve (I_D-V_{BG}), (**B**) double sweep electrical output curve (I_D-V_{DS}) and (**C**) sensor response test to 10 ppm H_2S, 0.5% H_2 and 100 ppm NO_2 in air.

S2. Nanoparticle sensing layer sparsity analysis

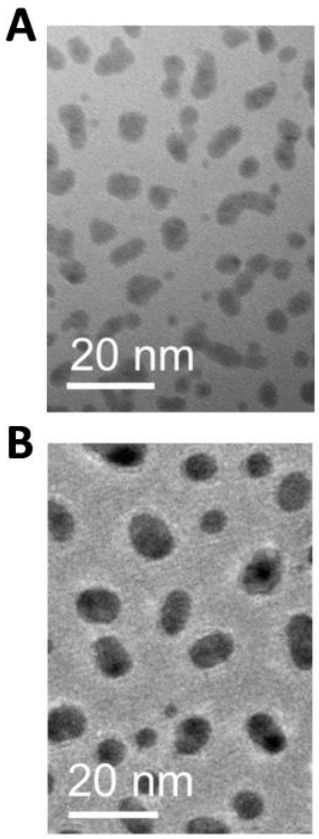

fig. S2. Top-down TEM image of an ultrathin $Pd_{0.3nm}Au_{1nm}$ on Si_3N_4 grids. (**A**) as-deposited and (**B**) air-annealed at 250^{o}C for 1 minute.

S3. Effect of silicon channel thickness on CS-FET sensitivity

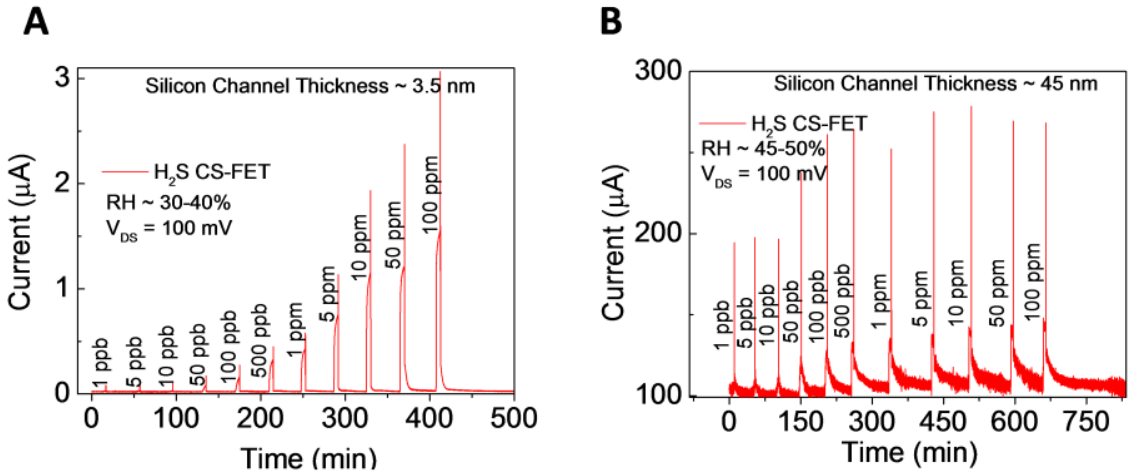

fig. S3. CS-FET sensor response dependence on silicon channel thickness. (**A**) High sensitivity from 3.5 nm thin silicon channel and (**B**) low sensitivity from 45 nm thick silicon channel Pd-Au CS-FET (H_2S sensor).

S4. CS-FET sensor response to temperature, relative humidity, and room temperature recovery characteristics

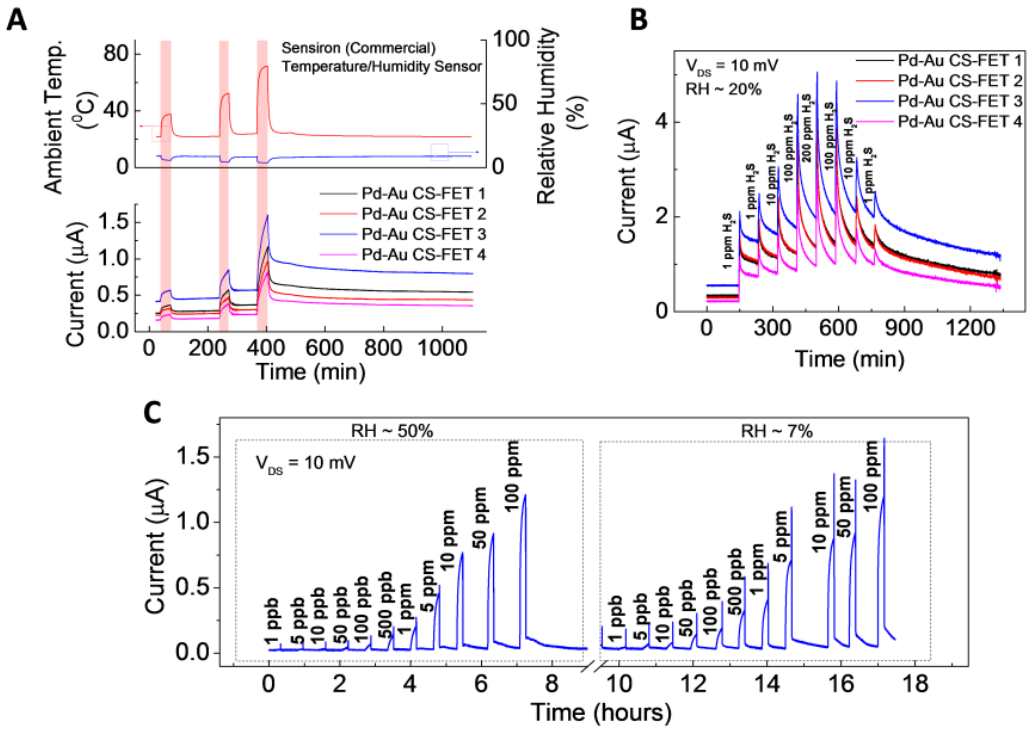

fig. S4. Influence of ambient temperature and humidity on CS-FET sensor response. (**A**) Effect of ambient temperature on Pd-Au based H_2S CS-FET characteristics (V_{DS} = 10 mV, V_{BG} = 0 V, RH ~ 20%, T ~ 25°C), (**B**) un-assisted, room temperature recovery from H_2S in Pd-Au CS-FET and (**C**) influence of humidity on a Pd-Au based H_2S sensitive CS-FET.

S5. Individual sensor cycling from low and high gas concentrations

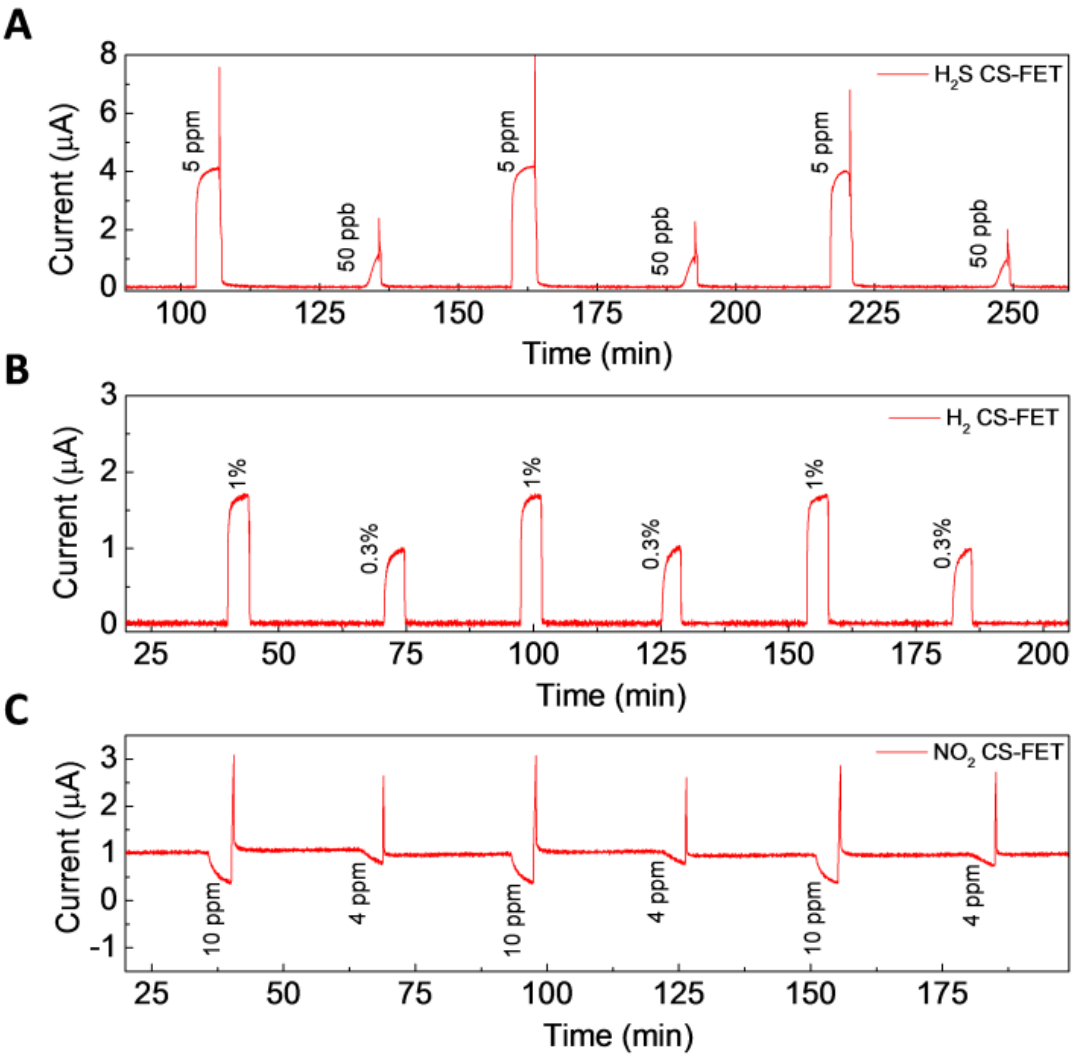

fig. S5. High-low-high gas concentration cycling of CS-FET sensors. (**A**) Pd-Au based H2S CS-FET (V_{DS} = 1 V, V_{BG} = 0 V, RH ~ 25-35%, T ~ 25ºC), (**B**) Ni-Pd based H2 CS-FET (V_{DS} = 100 mV, V_{BG} = 0 V, RH ~ 25-35%, T ~ 25ºC) and (**C**) Ni based NO2 CS-FET (V_{DS} = 1 V, V_{BG} = 10 V RH ~ 25-35%, T ~ 25ºC). [Experiments were carried out using CS-FET sensors made using SOI wafers procured from Shin-Etsu, Japan – see Materials and Methods section for more details].

S6. Fabrication process of chemical-sensitive 3.5-nm-thin silicon transistors

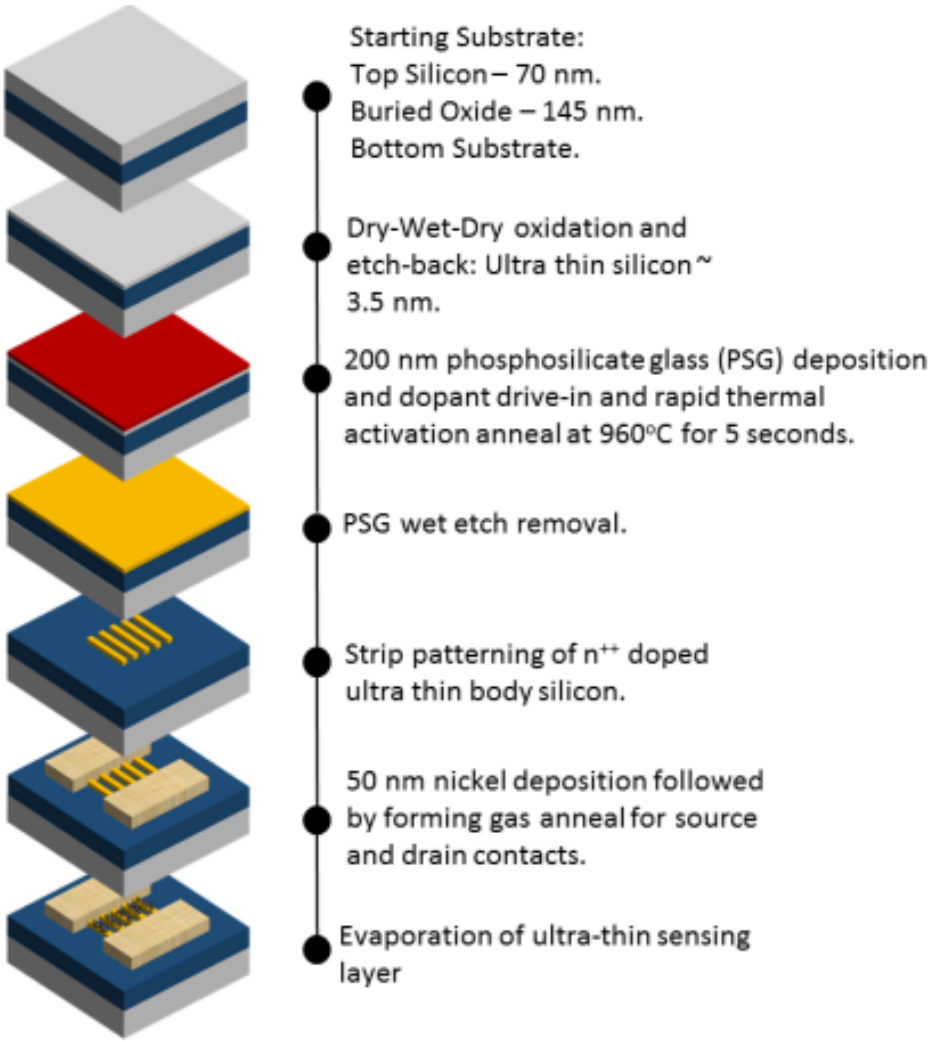

fig. S6. CMOS-compatible fabrication process of CS-FETs.

S7. Microheater characterization

In order to identify a reasonable choice of µ-Heater materials, we investigated a few well known low resistance thin-film materials with the capability to offer sufficient heating without breakdown. From the I-V characteristics in supplementary fig. S7, Au/Cr and Cu are the best in terms of low resistance materials offering higher temperature heating at relatively lower voltage and hence power. Cu as a thin-film heater material was not used on account of its instability at higher temperatures with a tendency to breakdown (burn-out) after repeated heating cycles. Furthermore, Cu tends to be highly reactive with sulfur containing gases making it unsuitable for recovery from corrosive gases like H_2S. Based on this, Au/Cr was used as the µ-Heater material. Supplementary fig. S7B depicts the optical characterization of a single Au (200 nm)/Cr (20 nm) in the dual µ-Heater arrangement using infra-red (IR) microscopy. In order to correlate this with the approximate local surface temperature, one of the µ-Heaters in the dual µ-Heater configuration was used as a temperature sensor. This way the surface temperature around the CS-FET due to heat radiated by a single µ -heater could be approximated and correlated with the IR data. Supplementary fig. S7C shows the calibrated Au (200 nm)/Cr (20 nm) temperature sensor reading due to heat radiated from the adjacent µ-Heater (inset shows the linearity of the temperature sensor). In the final configuration of the CS-FET chip, thicker Au (400 nm)/Cr (20 nm) was used as the heater material to achieve a relatively lower operative voltage affording higher heating temperatures for sensor recovery. In all time-dependent sensor measurements, a recovery temperature ~ 200 ^{o}C was used for 5-30 seconds corresponding to ~ 100 mA from a single µ-heater made of Au (400 nm) / Cr (20 nm). Better choice of µ-Heater materials, pattern design and placement can be made to minimize heat loss, thereby lowering µ-heater power consumption.

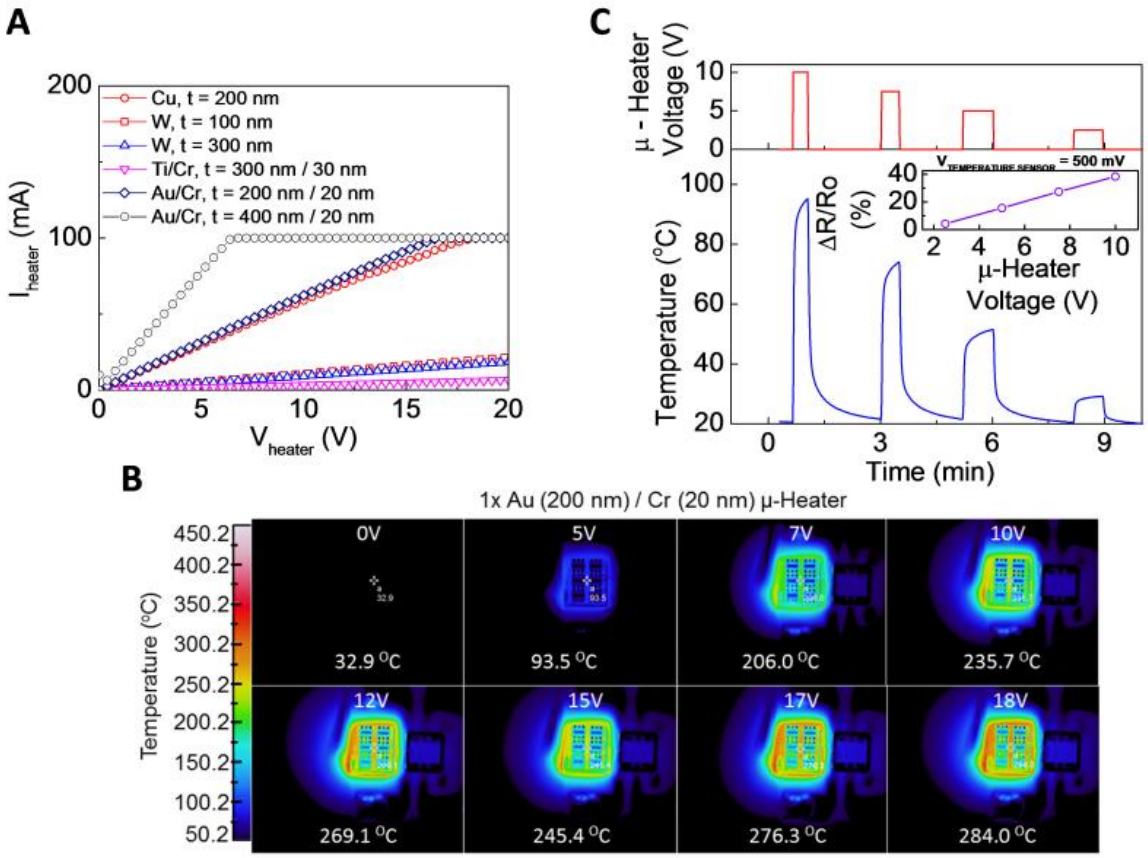

fig. S7. Integrated microheater material selection and characterization. (**A**) I-V characteristics of micro-heater (μ-Heater) with different materials and thicknesses, (**B**) infra-red (IR) characterization of a single Au (200 nm) / Cr (20 nm) μ-Heater and (**C**) Local surface temperature characterization due to radiated heat from a single Au (200 nm) / Cr (20 nm) μ-Heater around the vicinity of the CS-FET, using the adjacent μ-Heater (from the dual heater arrangement) as a single temperature sensor (Inset: Linearity of the temperature sensor; sensitivity vs dissipated heat from adjacent μ-Heater.

S8. Transfer characteristics of H_2S, H_2, and NO_2 CS-FETs

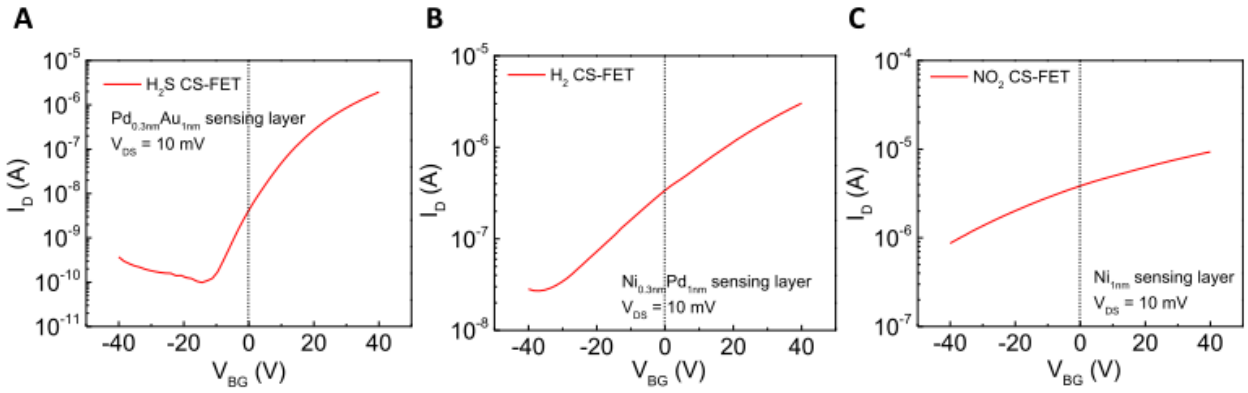

fig. S8. Typical electrical transfer characteristics (I_D-V_{BG}) of functionalized CS-FETs. (**A**) Pd-Au CS-FET for H_2S detection, (**B**) Ni-Pd CS-FET for H_2 detection and (**C**) Ni CS-FET for NO_2 detection.